Supporting Information for

Unraveling interlayer coupling effect on layer-dependent electronic and optoelectronic properties in two-dimensional semiconductors

Zeqi Hua,[a] Haibo Shu,[a,b,*] Dabao Xie,[a] Zehao Liu,[a] Jiayu Liang,[a,*] Jing Zhou,[b] Xiaoshuang Chen,[b] and Dan Cao[c]

[a] College of Optical and Electronic Technology, China Jiliang University, Hangzhou 310018, China.

[b] State Key Laboratory of Infrared Physics, Shanghai Institute of Technical Physics, Chinese Academy of Science, Shanghai 200083, China

[c] College of Science, China Jiliang University, Hangzhou 310018, China

[*]Corresponding author. Email: shuhaibo@cjlu.edu.cn, jyliang513@cjlu.edu.cn

CONTENTS

S1. Vacuum-layer-dependent absorption spectra and absorptivity

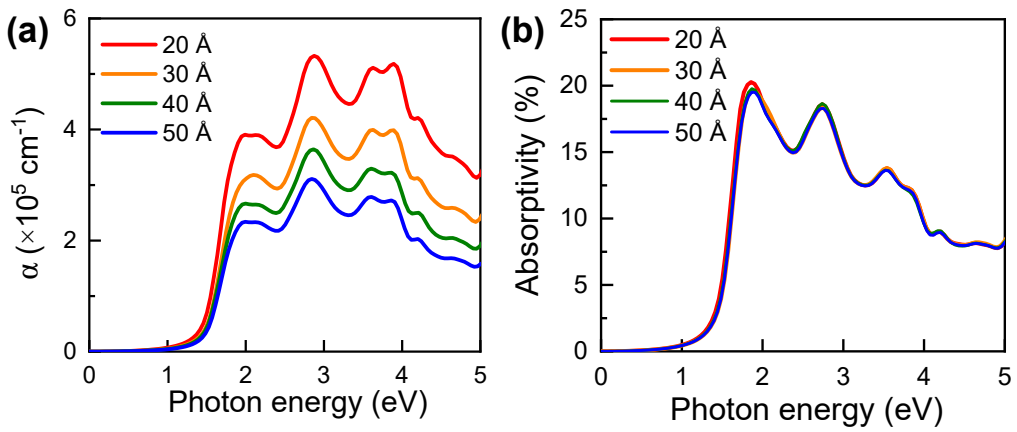

Fig. S1 (a) Absorption spectra and (b) absorptivity of monolayer $PtSe_2$ with different thicknesses (20~50 Å) of vaccum layer in the calculated models.

S2. Lattice and energetic parameters of 2D semiconductors

Table S1. In-plane lattice parameters (a and b), interlayer distance (d_{int}), and interlayer binding energy (E_b) of eighteen 2D semiconductors.

Materials	a (Å)	b (Å)	d_{int} (Å)	E_b (meV/Å^2)
PtS_2	3.56	3.56	2.32	31.7
$PtSe_2$	3.75	3.75	2.27	35.7
HfS_2	3.64	3.64	3.01	21.9
$HfSe_2$	3.76	3.76	3.13	22.3
TiS_2	3.40	3.40	2.87	24.8
$TiSe_2$	3.52	3.52	3.00	26.8
WS_2	3.18	3.18	3.10	26.1
WSe_2	3.31	3.31	3.18	25.6
MoS_2	3.18	3.18	3.04	25.2
$MoSe_2$	3.32	3.32	3.18	27.1
$MoTe_2$	3.55	3.55	3.33	26.1
ReS_2	6.41	6.51	3.63	21.1
$ReSe_2$	6.65	6.78	3.41	23.1
SnS	4.07	4.31	3.63	29.3
SnSe	4.29	4.41	2.74	30.1
GeS	3.62	4.57	2.65	29.7
GeSe	3.98	4.26	2.94	29.2
BP	4.63	3.30	3.11	33.4

S3. Comparison of interlayer binding energy of 2D semiconductors between this work and previous studies

Table S2 Comparison of interlayer binding energy (E_b) of 2D semiconductors between this work and previous reports.

Materials	Methods	E_b (meV/Å^2)	References
BP	DFT-D3	33.4	This work
	optB88-vdW	29.9	1
	PBE	38.2	2
MoS_2	DFT-D3	25.2	This work
	optB88-vdW	24.2	1
	DFT-D3	27.1	3
$MoSe_2$	DFT-D3	27.1	This work
	Experiment	22.2	4
$MoTe_2$	DFT-D3	26.1	This work
	PBE	23.1	2
WS_2	DFT-D3	26.1	This work
	DFT-D3	27.9	3
GeS	DFT-D3	29.7	This work
	vdW-DF2	28.4	5
	DFT-D2	32.5	6
GeSe	DFT-D3	29.2	This work
	PBE	31.9	2
	DFT-D2	28.1	6
	vdW-DF2	30.8	5
SnSe	DFT-D3	30.1	This work
	optB88-vdW	32.1	1

S4. Comparison of interlayer binding energy and interlayer distance between the bilayer and bulk van der Waals crystals

Table S3 Comparison of interlayer binding energy (E_b) and interlayer distance (d_{int}) in twelve van der Waals crystals with bilayer and bulk structures.

Materials	Bilayer		Bulk	
	E_b (meV/Å^2)	d_{int} (Å)	E_b (meV/Å^2)	d_{int} (Å)
$PtSe_2$	35.7	2.27	37.6	2.19
$HfSe_2$	22.3	3.13	23.3	3.04
WS_2	26.1	3.18	28.8	3.07
MoS_2	25.2	3.18	27.2	3.09
ReS_2	21.1	3.63	25.2	3.42
$ReSe_2$	23.1	3.41	26.5	3.32
SnS	29.3	2.63	30.2	2.61
SnSe	30.1	2.74	30.8	2.67
GeS	29.7	2.65	30.3	2.61
GeSe	29.2	2.94	30.0	2.66
BP	33.4	3.11	37.4	3.08
Graphene	16.6	3.54	17.9	3.47

S5. Projected band structures of trilayer $PtSe_2$ and $HfSe_2$

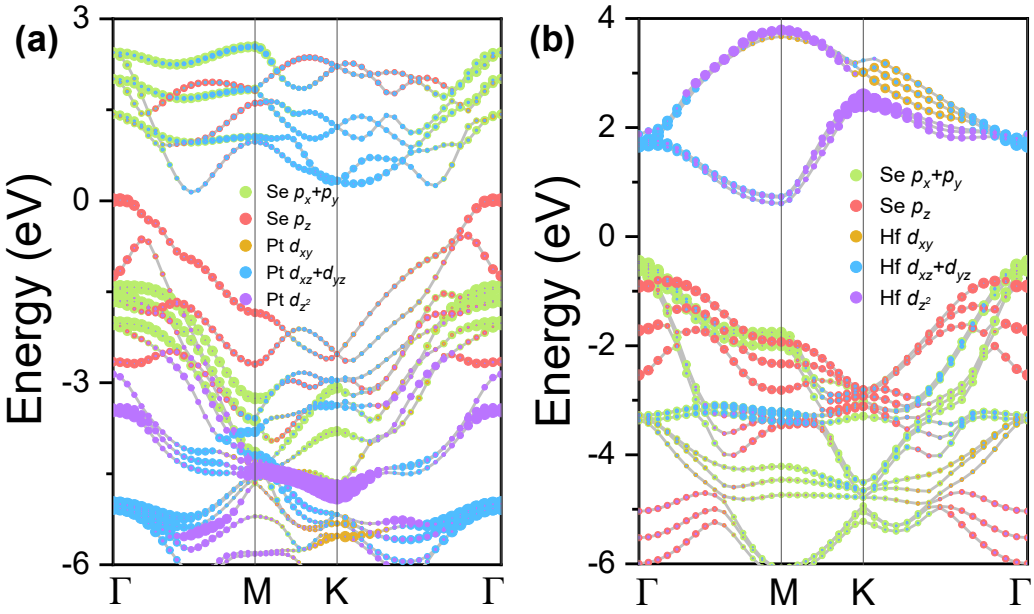

Fig. S2 Projected band structure of (a) 3L-$PtSe_2$ and (b) 3L-$HfSe_2$. The Fermi level position is set to energy zero point.

S6. Projected density of states of 2D $PtSe_2$ and $HfSe_2$

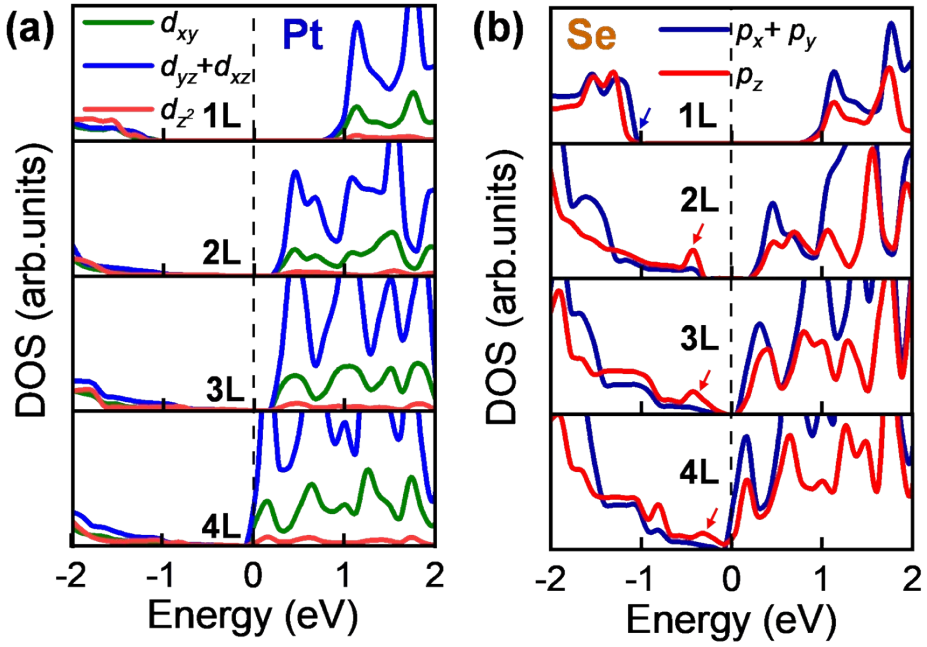

Fig. S3 Projected density of states of (a) Pt and (b) Se atoms in 2D $PtSe_2$ with the range of layer number from 1L to 4L. The dash lines denote the position of Fermi level.

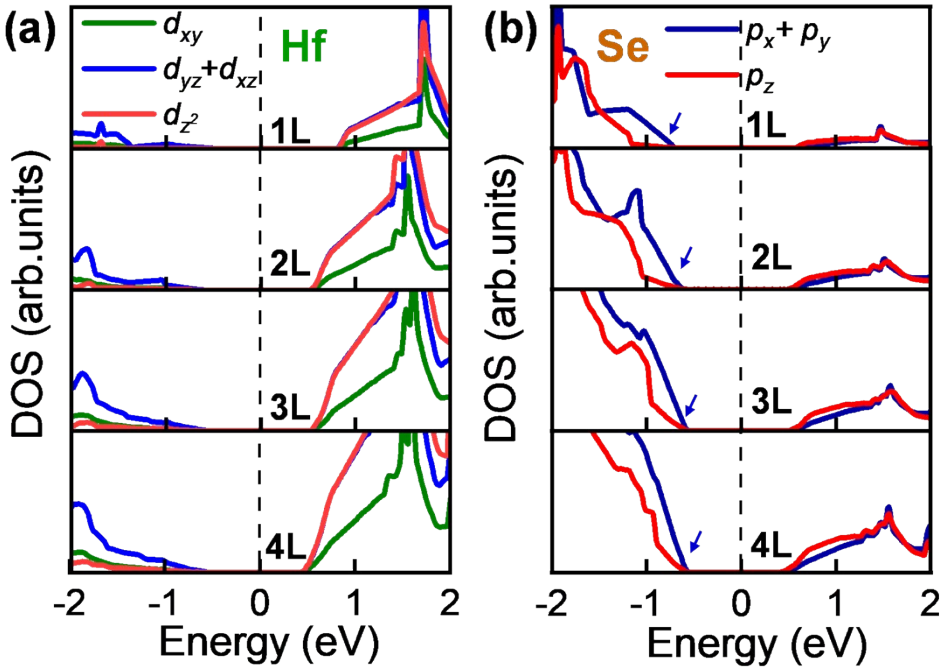

Fig. S4 Projected density of states of (a) Hf and (b) Se atoms in 2D $HfSe_2$ with the range of layer number from 1L to 4L. The dash lines denote the position of Fermi level.

S7. Transmission spectra of 2D $PtSe_2$ and $HfSe_2$ devices

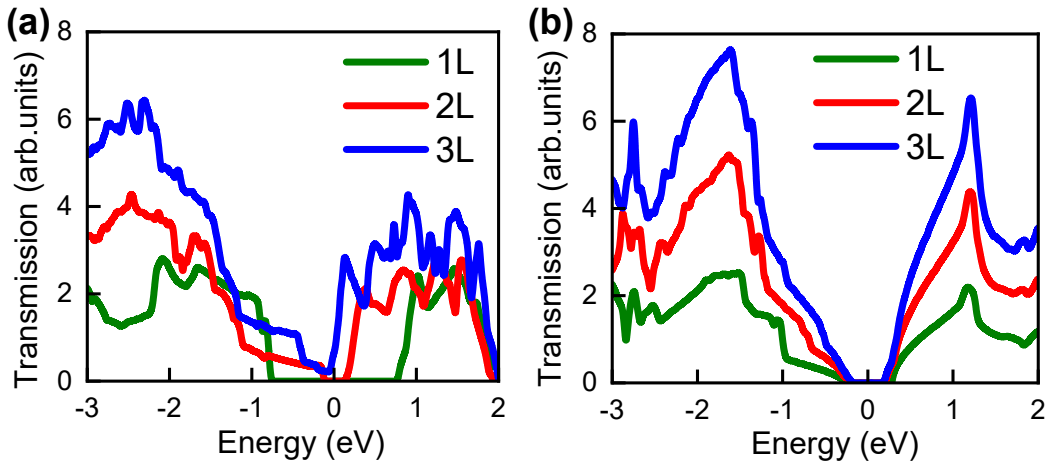

Fig. S5 Transmission spectra of 2D (a) $PtSe_2$ and (b) $HfSe_2$ devices with the range of layer number from 1L to 3L.

S8. Polarized photocurrent of 2D $PtSe_2$ and $HfSe_2$ under different photon energies

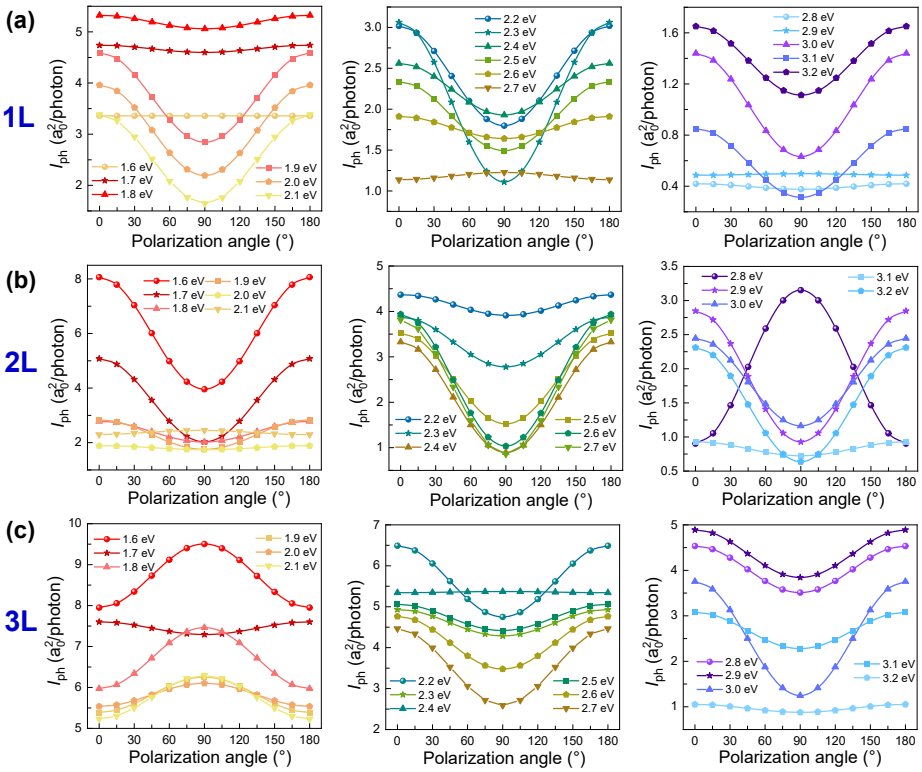

Fig. S6 The polarized I_{ph} of (a) 1L-$PtSe_2$, (b) 2L-$PtSe_2$, and (c) 3L-$PtSe_2$ devices as a function of polarization angle under different photon energies.

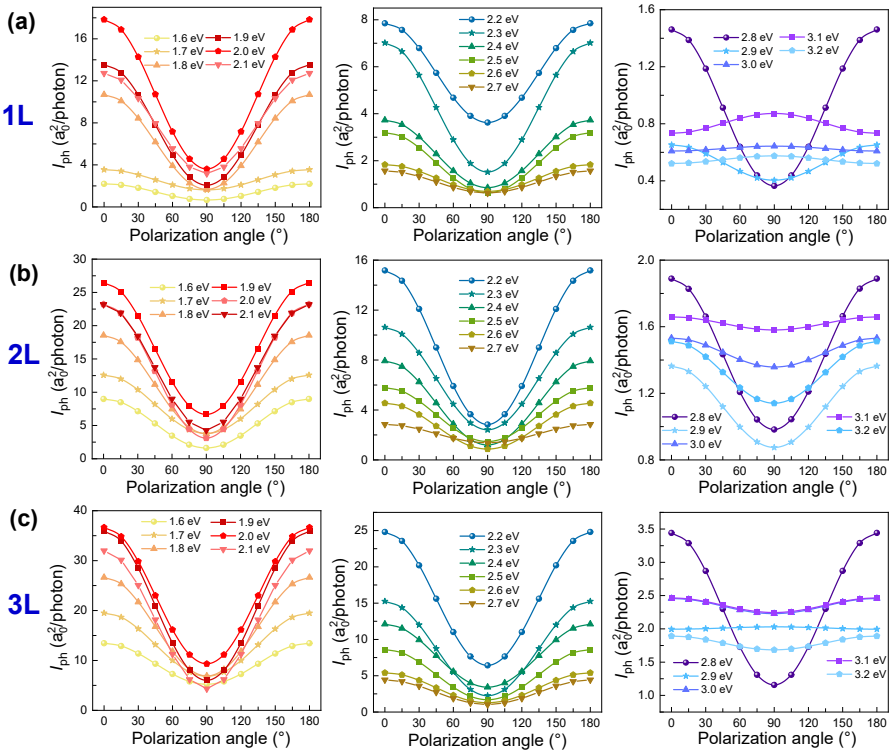

Fig. S7 The polarized I_{ph} of (a) 1L-$HfSe_2$, (b) 2LHfSe_2, and (c) 3L-$HfSe_2$ devices as a function of polarization angle under different photon energies.

References

1 L.-C. Zhang, G. Qin, W.-Z. Fang, H.-J. Cui, Q.-R. Zheng, Q.-B. Yan and G. Su, *Sci. Rep.*, 2016, **6**, 19830.

2 N. Karmodak and O. Andreussi, *ACS Energy Lett.*, 2020, **5**, 885–891.

3 J. Liu, T. Shen, J.-C. Ren, S. Li and W. Liu, *Applied Surface Science*, 2023, **608**, 155163.

4 E. Blundo, T. Yildirim, G. Pettinari and A. Polimeni, *Phys. Rev. Lett.*, 2021, **127**, 046101.

5 S. P. Poudel, J. W. Villanova and S. Barraza-Lopez, *Phys. Rev. Mater.*, 2019, **3**, 124004.

6 X. Lv, W. Wei, Q. Sun, F. Li, B. Huang and Y. Dai, *Appl. Catal. B: Environ.*, 2017, **217**, 275–284.